Journal of Radiation Research, Vol. 63, No. S1, 2022, pp. i26–i37
https://doi.org/10.1093/jrr/rrac045
Review Article

Pathological observation of the effects of exposure to radioactive microparticles on experimental animals

Kazuko Shichijo[1,*] and Toshihiro Takatsuji[2]

[1]Department of Tumor and Diagnostic Pathology, Atomic Bomb Disease Institute, Nagasaki University, 1-12-4 Sakamoto, Nagasaki 852-8523, Japan
[2]Faculty of Environmental Studies, Nagasaki University, Bunkyo 1-14, Nagasaki 852-8521, Japan
*Corresponding author. Department of Tumor and Diagnostic Pathology, Atomic Bomb Disease Institute, Nagasaki University, 112-4 Sakamoto, Nagasaki 852-8523, Japan. Tel.: +81-95-819-7107; Fax: +81-95-819-7108; E-mail: shichijo@nagasaki-u.ac.jp
(Received 5 November 2021; revised 22 January 2022; editorial decision 17 June 2022)

ABSTRACT

Internal radiation exposure from neutron-induced radioisotopes that were environmentally activated following an atomic bombing or nuclear accident should be considered for a complete picture of the pathologic effects on survivors. Inhaled hot particles expose neighboring tissues to very high doses of particle beams, which can cause local tissue damage. Experimentally, a few μm of $^{55}MnO_2$ powder was irradiated with neutrons at a nuclear reactor in order to generate $^{56}MnO_2$ that emits β-rays. Rats were irradiated via inhalation. Pathological changes in various rat tissues were examined. In addition, the ^{56}Mn β energy spectrum around the particles was calculated to determine the local dose rate and the cumulative dose. This review focuses on our latest pathological findings in lungs with internal radiation injury and discusses the pathological changes of early event damage caused by localized, very high-dose internal radiation exposure, including apoptosis, elastin stigma, emphysema, hemorrhage and severe inflammation. The pathological findings of lung tissue due to internal radiation exposure of 0.1 Gy were severe, with no pathological changes observed due to external exposure to γ radiation at a dose of 2.0 Gy. Therefore, it is suggested that new pathological analysis methods for internal exposure due to radioactive microparticles are required.

Keywords: radioactive particle; internal radiation exposure; pathology; lung; atomic bombing; elastin

INTRODUCTION

To fully understand the radiation effects on survivors of the Hiroshima and Nagasaki atomic bombings (A-bombs), as well as victims of nuclear disasters such as nuclear power plant accidents, one must consider not only the initial radiation received directly from the bombs and/or other sources, but also that received from neutron-induced radioisotopes in soil, dust and so on, as well as radiation from dispersed fission products and nuclear fuel materials. Among these, radioactive particles dispersed in the air (radioactive dust) can be a source of internal exposure. In assessing the radiation risk of those who moved to the affected area shortly after an explosion or other nuclear disaster, inhalation of radioactive dust may be more important than external exposure. In Hiroshima, Otani *et al.* suggested the possibility of radioactive dust exposure from the study of early entrants into Hiroshima following the explosion [1]. There is further evidence of dust falling following the attack in the Nagasaki area [2].

There are two types of radioactivity derived from atomic bombs: (i) fission products such as ^{137}Cs and ^{90}Sr and fuel components such as Pu [3], and (ii) induced radioactivity produced by neutron irradiation of soil such as ^{56}Mn and ^{24}Na. Because most nuclides have short half-lives, neutron-induced radioactivity has received little attention. While the International Atomic Energy Agency (IAEA) recently featured a coordinated study on radioactive particles focusing on environmental fate and transfer into the body [4], we conducted a study to investigate biological effects [5, 6]. For radioactive microparticles in soluble form, irradiation dose is thought to be distributed similarly to external exposure [7, 8]. However, our estimates indicate extremely high-dose rates in the vicinity of insoluble radioactive microparticles.

Because neutrons generated in the process of an atomic bomb explosion or nuclear accident have no electric charge, they can enter the nuclei of atoms very easily without being disturbed by the Coulomb force, and they often create unstable nuclei—radionuclides—with one extra neutron (neutron activation). The resulting radioactive material generates radioactive particles, which can cause internal radiation exposure by inhalation. In many cases, tissues in contact with inhaled radioactive particles are locally exposed to very high doses of radiation

from β rays, characteristic X-rays and Auger electrons. These effects must be taken into account in order to obtain a complete picture of the radiopathological effects on survivors.

In terms of internal radiation exposure to the human body, we have already reported Pu deposits in the bodies of Nagasaki A-bomb victims. The average dose of Pu in the Nagasaki A-bomb victims' organs was evaluated over their survival period, and it was shown to be lower when compared to external exposure. However, the impact of a single α-particle on an individual cell nucleus should not be overlooked, and it would be meaningful to investigate the relationship between the impact of internal exposure on the cellular level dose and the organ average dose [9–11]. When comparing the same tissue average dose, internal exposure has been shown to have a greater effect than external exposure [12]. In 1986, the Chernobyl nuclear power plant accident exposed residents of Ukraine, Belarus and Russia to radioactive iodine, particularly infants and children who drank milk from cows that had eaten hay and other food sources contaminated with radioactive fallout [13]. In 2011, it was claimed that radioactive particles (cesium balls) were scattered in the air during the Fukushima Daiichi Nuclear Power Plant accident, which was triggered by the Great East Japan Earthquake [14].

This review focuses on the pathological effects of ^{56}Mn microparticles on the lung. It is well known that radiation exposure of the lungs can induce 'radiation pneumonitis' in laboratory animals at lung doses of more than 8 Gy of low linear energy transfer (LET) radiation [15, 16]. In rats, studies showed that a 20 Gy thorax irradiation did not induce any short-term histological changes in the lungs, while the irradiated lungs developed focal exudative lesions after 2 months and reparative fibrotic lesions after 6 months [17, 18]. In addition, lung function was impaired by irradiation with a single dose of 12 Gy [19]. Our experiments showed that internal exposure to a tissue-averaged dose of 0.10 Gy (Table 1) caused serious pathological changes in the lungs compared to 2 Gy of ^{60}Co external exposure.

We have conducted a series of internal radiation exposure experiments on animals in order to study the effects of radioactive particles, including their initial effects and subsequent pathological profiles, and we found that inhaling radioactive microparticles can cause serious radiation damage due to localized exposure to very high doses, even if the average dose is low (Fig. 1). Microdistribution of internal radiation dose in lung tissues exposed to ^{56}Mn dioxide microparticles has been reported [6, 20]. The detection of the three-dimensional spatial distribution of the radiation effects of radioactive particles embedded in tissues, as well as the analysis of their relationship to the microscopic dose distribution around the radioactive particles, will be important for the study of internal exposure. This entails linking the microdistribution of internal radiation dose in biological tissues to pathobiological effects.

EXPOSURE TO 0.1 GY INTERNAL RADIATION CAUSES MUCH MORE PATHOLOGICAL CHANGES THAN EXTERNAL EXPOSURE TO Γ RADIATION AT A DOSE OF 2.0 GY

A nuclear reactor activates nonradioactive manganese-55 dioxide ($^{55}MnO_2$) powder to produce $^{56}MnO_2$ powder, which emits β rays (activated powder). The pathological effects of internal exposure to radiation via activated powder inhalation on male Wistar rats were compared to those of external exposure to γ-rays. ^{56}Mn is one of the major radioisotopes generated in soil by neutron irradiation from atomic bomb explosions and is responsible for exposure (DS86 Vol. 1 [21]). Since ^{56}Mn has a short physical half-life of 2.58 hours, exposure to it is largely restricted to the first few hours following inhalation.

The MnO_2 powder particles used in this experiment were the same size as previously reported, with a diameter of approximately 5 μm [22, 23]. The activated powder was produced by neutron irradiation of 100 mg of $^{55}MnO_2$ powder (Rare Metallics, Japan) in the IVG.1 M ('Baikal-1') reactor in Kurchatov, Kazakhstan (page 110 of [24]). The irradiating neutrons had a particle fluence of 4×10^{14} n/cm^2 per 2000 seconds of irradiation time, which was irradiated for 2000 (1×), 4000 (2×) and 8000 (4×) seconds to produce three types of activated powders [22].

The radioactivity of this activated powder with ^{56}Mn was 2.74×10^8 Bq, $2 \times 2.74 \times 10^8$ Bq and $4 \times 2.74 \times 10^8$ Bq for the whole 100 mg for 1×, 2× and 4×, respectively. This was pneumatically sprayed onto the rats in the experimental box. On the other hand, γ-irradiation was performed using a Teragam K2 unit (UJP Praha, Praha-Zbraslav, Czech Republic), which externally irradiated rats with 2.0 Gy of ^{60}Co γ-rays at a dose rate of 2.6 Gy/min, which is the dose of fractionated radiation therapy with low LET radiation that falls on the shoulder of the cell survival curve and maximizes sublethal damage repair and repopulation of the normal tissue. In addition, a control group that was neither exposed to activated powder nor γ-irradiation (unexposed control group) [6] and a group that inhaled nonactivated MnO_2 powder (stable Mn) [6] were established.

The pathological effects of internal exposure to radiation were emphysema, hemorrhage and severe inflammation, all of which were reported 6 hours to 8 months after the exposure, during which bronchial epithelial cell apoptosis was also found [6].

The initial pathological findings and damage to the lung tissue from 0.1 Gy internal radiation exposure were nonspecific, more rapid and more severe than in the external exposure group to 2.0 Gy of γ rays (externally exposed or γ 2.0 Gy group) [6], the unexposed control group and the stable Mn group. Pathological changes such as emphysema and hemorrhage were observed in the lungs of rats exposed to 1× radioactive powder ($1 \times 2.74 \times 10^8$ Bq) and severe inflammation was observed and persisted in the groups exposed to 4× and 2× ($2 \times 2.74 \times 10^8$ Bq) radioactive powder (internally exposed ^{56}Mn (4×) and (2×) groups) [6] 6 hours to 6 months after the exposure. These changes were more pronounced in the group internally exposed to 4× activated powder ($4 \times 2.74 \times 10^8$ Bq). The lung tissue damage observed on the third day of internal exposure to 4× and 2× ($2 \times 2.74 \times 10^8$ Bq) radioactive powders persisted in these same rat groups 6 months after exposure (Tables 1, 2, Figs 2–4).

Collagen fiber deposition, which has been traditionally used as an indicator of fibrosis in radiation-induced pneumonitis, was low in the internally exposed 2× group. On the other hand, elastic fibers (elastin) demonstrated an abnormally localized high deposition surrounding the alveoli 6 hours after internal radiation exposure, with a staggered distribution that was cut off at intervals (elastin stigma), as if a bullet (shot) had been fired (Fig. 5A). External exposure to γ radiation at 2.0 Gy had a similar effect, but at a lower deposition level compared to the 4× activated powder, and this effect was normalized to control

Table 1. The ^{56}Mn specific activities A_0 and tissue average cumulative absorbed doses D of internal irradiation in various organs and tissues of experimental rats [6]

	^{56}Mn(1×)		^{56}Mn(2×)		^{56}Mn(4×)	
	A_0 (kBq/g)	D (Gy)	A_0 (kBq/g)	D (Gy)	A_0 (kBq/g)	D (Gy)
Liver	4.14 ± 0.35	0.015 ± 0.001	1.40 ± 0.33	0.005 ± 0.001	3.00 ± 0.70	0.011 ± 0.003
Heart	5.46 ± 0.60	0.016 ± 0.021	2.00 ± 0.30	0.006 ± 0.001	4.50 ± 0.94	0.014 ± 0.004
Kidney	3.97 ± 0.48	0.013 ± 0.002	2.30 ± 0.51	0.008 ± 0.002	3.60 ± 0.60	0.012 ± 0.003
Tongue	45.0 ± 5.4	0.069 ± 0.011	12.0 ± 2.8	0.018 ± 0.005	28.0 ± 5.0	0.043 ± 0.012
Lungs	71.8 ± 9.3	0.100 ± 0.014	37 ± 7	0.051 ± 0.011	81 ± 13	0.110 ± 0.023
Esophagus	25.5 ± 3.6	0.050 ± 0.009	6.4 ± 1.6	0.012 ± 0.003	16 ± 3.3	0.030 ± 0.007
Stomach	148 ± 16	0.24 ± 0.03	140 ± 28	0.22 ± 0.06	210 ± 47	0.33 ± 0.08
Small intestine	811 ± 93	1.33 ± 0.17	350 ± 79	0.58 ± 0.14	890 ± 210	1.48 ± 0.37
Large intestine	1011 ± 100	1.65 ± 0.18	410 ± 87	0.69 ± 0.17	1160 ± 270	1.90 ± 0.47
Trachea	5.79 ± 0.75	0.014 ± 0.002	3.90 ± 0.77	0.010 ± 0.002	6.50 ± 1.40	0.016 ± 0.004
Eyes	13.2 ± 1.7	0.021 ± 0.003	19.0 ± 4.4	0.031 ± 0.008	24.0 ± 5.3	0.004 ± 0.010
Skin	40.6 ± 4.9	0.076 ± 0.010	45.0 ± 8.2	0.086 ± 0.020	49.0 ± 9.0	0.095 ± 0.020
Whole body	83.4 ± 11.0	0.150 ± 0.025	51.0 ± 11.0	0.091 ± 0.026	77.0 ± 15.0	0.140 ± 0.030

^{56}Mn(1×); Initial total activity of 100 mg $^{56}MnO_2$ powder sprayed was 2.74×10^8 Bq [22].
^{56}Mn(2×); Initial total activity of 100 mg $^{56}MnO_2$ powder sprayed was 5.48×10^8 Bq.
^{56}Mn(4×); Initial total activity of 100 mg $^{56}MnO_2$ powder sprayed was 1.10×10^9 Bq.

Table 2. Histological findings in the lungs of rats in the internally exposed ^{56}Mn, 2.0 Gy γ externally exposed and unexposed control groups [6]

Group		Hour6		Day3		Day14		Month2		Month6		Group	Month8	
Hemorrhage	^{56}Mn(4×)	3[a)]	(+∼++)[b)]	3	(++∼+++)	2	(+)	3	(+∼++)	4	(+∼+++)	^{56}Mn(1×)	6	(++∼+++)
Emphysema		2	(++∼+++)	2	(++)	2	(+∼++)	3	(+∼++)	4	(+∼++)		6	(++∼+++)
Inflammation		3	(+∼+++)	3	(++)	2	(+∼++)	3	(+∼+++)	4	(++∼+++)		6	(++∼+++)
Atelectasis		0	(−)	0	(−)	0	(−)	0	(−)	2	(++∼+++)		3	(++∼+++)
Pneumonia		0	(−)	0	(−)	0	(−)	0	(−)	1	(+)		0	(−)
Granuloma		0	(−)	0	(−)	0	(−)	0	(−)	1	(+)		0	(−)
		(n = 3)		(*n* = 3)		(*n* = 3)		(*n* = 3)		(*n* = 4)			(*n* = 6)	
Hemorrhage	^{56}Mn(2×)	3	(+∼++)	3	(++∼+++)	2	(+∼++)	3	(++)	2	(+∼++)	Mn	1	(+)
Emphysema		2	(+)	3	(+∼++)	3	(+∼+++)	3	(+∼++)	2	(+∼++)	stable	1	(+++)
Inflammation		3	(+∼++)	3	(++∼+++)	3	(+∼+++)	3	(++)	2	(++∼+++)		1	(+)
Atelectasis		0	(−)	1	(++)	0	(−)	0	(−)	1	(+)		1	(−)
Pneumonia		0	(−)	0	(−)	0	(−)	0	(−)	1	(+)		0	(−)
Granuloma		0	(−)	0	(−)	0	(−)	0	(−)	0	(−)		0	(−)
		(*n* = 3)		(*n* = 3)		(*n* = 3)		(*n* = 3)		(*n* = 3)			(*n* = 4)	
Hemorrhage	γ 2.0 Gy	3	(+∼++)	0	(−)	1	(+)	1	(+)	1	(+)	γ 2.0Gy	1	(++)
Emphysema		2	(+∼++)	2	(+)	0	(−)	1	(+)	0	(−)		2	(+)
Inflammation		3	(+)	1	(+)	1	(+)	1	(+)	1	(+)		2	(+∼+++)
Atelectasis		0	(−)	0	(−)	0	(−)	0	(−)	0	(−)		1	(+)
Pneumonia		0	(−)	0	(−)	0	(−)	0	(−)	0	(−)		0	(−)
Granuloma		0	(−)	0	(−)	0	(−)	0	(−)	0	(−)		0	(−)
		(*n* = 3)		(*n* = 3)		(*n* = 3)		(*n* = 3)		(*n* = 4)			(*n* = 4)	
Hemorrhage	Control	0	(−)	0	(−)	0	(−)	0	(−)	0	(−)	Control	0	(−)
Emphysema		0	(−)	1	(+)	0	(−)	0	(−)	0	(−)		1	(+)
Inflammation		1	(+)	1	(+)	0	(−)	1	(+)	0	(−)		0	(−)
Atelectasis		0	(−)	0	(−)	0	(−)	0	(−)	0	(−)		1	(+)
Pneumonia		0	(−)	0	(−)	0	(−)	0	(−)	0	(−)		0	(−)
Granuloma		0	(−)	0	(−)	0	(−)	0	(−)	0	(−)		0	(−)
		(*n* = 3)		(*n* = 3)		(*n* = 3)		(*n* = 3)		(*n* = 4)			(*n* = 5)	

Notes: [a)] the number of rats with incidence and pathologic grades (in parenthesis) and [b)] pathologic grades ranging from − to +++.

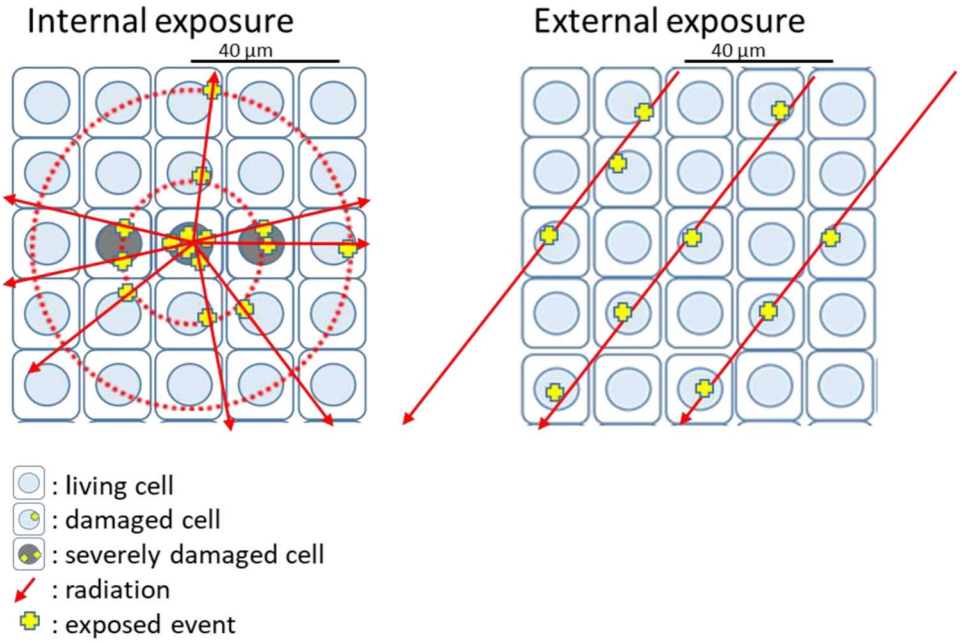

Fig. 1. A comparison between external exposure to high energy γ-ray and internal exposure to radioactive particles emitting β-ray. Near the radioactive particles, the radiation dose is high, and events caused by emitted electrons are concentrated. Therefore, multiple events occur in one cell nucleus, causing severe damage (left). On the other hand, exposure to an external γ-ray source results in a nearly uniform dose, and events occur relatively randomly as a result of photo-electrons and Compton electrons (right).

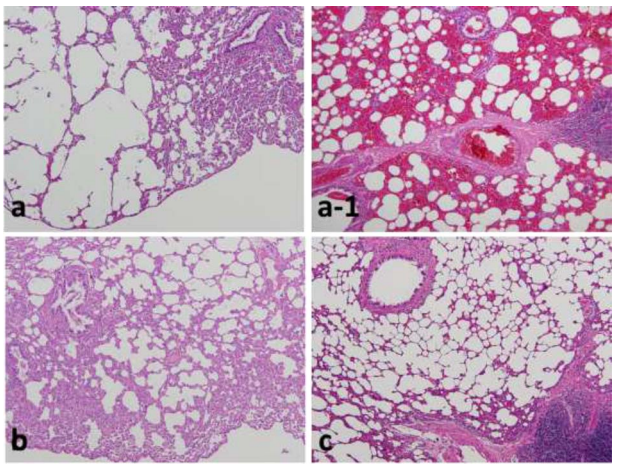

Fig. 2. Lungs of rats 3 days after exposure showing severe emphysema (a) and hemorrhage (a–1) in the ^{56}Mn internally exposed group (0.1 Gy), but no pathological changes in the ^{60}Co γ rays (2 Gy) externally exposed (b) and unexposed control groups (c). As with the control, experiments with a stable Mn group were also conducted, and no change was observed. Hematoxylin and eosin (H&E) staining, original magnification ×10. (a, a-1, c from [23]/CC BY 4.0).

levels after 3 days, but remained high for 6 months in the internally exposed (activated powder) groups.

Apoptotic cell death occurred in bronchial epithelial cells in the lungs of the internally exposed group 3 days, 14 days, 2 months and 8 months after the inhalations, but not in the externally exposed group (Figs 5A and D).

PATHOLOGICAL CHANGES DUE TO INTERNAL EXPOSURE WERE PERSISTENT

At 6 months, late pathological findings such as atelectasis, granuloma and severe pneumonitis were detected in the 2× and 4× radioactive powder internally exposed groups, with persistent tissue damage due to emphysema and long-term inflammation (Fig. 4, Table 2). Conventionally, the progressive alveolar wall thickening and emphysema detected in radiation-induced pneumonitis, as well as collagen deposition associated with fibrosis [25], were not observed in the case of internal radiation exposure.

In addition, elastin deposition—another pathological indicator of lung fibrosis—was found to be higher in the internally exposed group in our experiment, and this finding was cited as a 'new pathological indicator' of internal radiation exposure. Fujimoto *et al.* [26] found that elastin mRNA levels in the lung were higher in the internally exposed group than in the unexposed control and the 2 Gy externally exposed groups, with no significance. Therefore, further investigation of gene

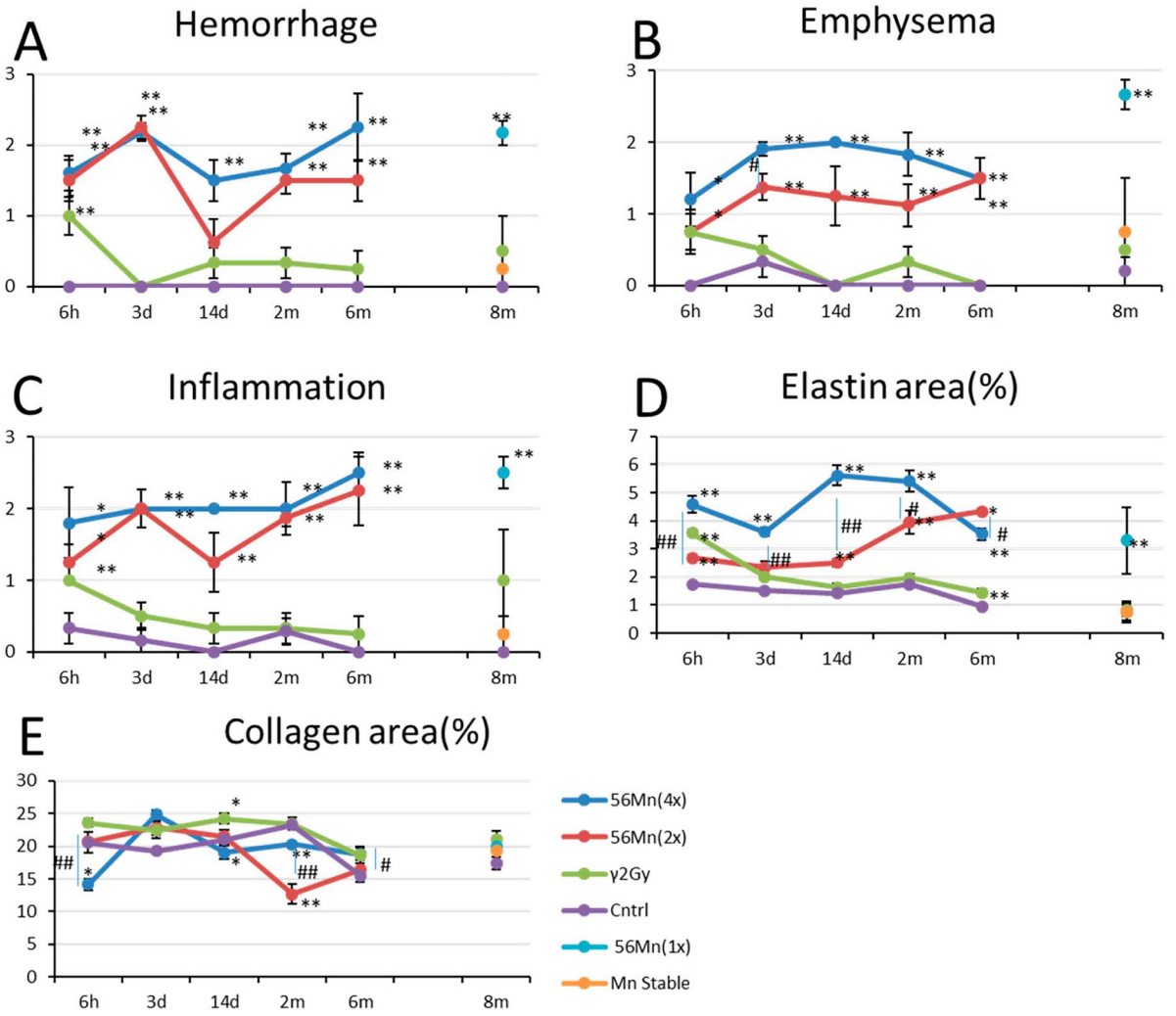

Fig. 3. Histologically-scored findings in the lungs of the rats exposed to stable Mn, ^{56}Mn, 2.0 Gy γ-radiation and no irradiation. (A) hemorrhage; (B) emphysema; (C) inflammation; (D) elastin; and (E) collagen findings in four groups: externally exposed, ^{56}Mn (2×) internally exposed, ^{56}Mn (4×) internally exposed and unexposed control and findings in 2.0 Gy γ-radiation externally exposed, stable Mn, ^{56}Mn (1×) internally exposed and unexposed control groups. Bars, mean ± standard error of the mean (SEM) (n = 3–6). $^{*}P < 0.05$, $^{**}P < 0.01$ vs control. $^{\#}P < 0.05$, $^{\#\#}P < 0.01$ vs ^{56}Mn (2×) [6].

expression is required. Internal exposure was also found to have long-term effects on locomotor activity in rats [27].

EARLY EFFECTS OF INTERNAL EXPOSURE FORESHADOW THE WARNING SIGNS (ELASTIN STIGMA) OF LATE EFFECTS

On Day 3, hemorrhage, emphysema and high score-level inflammation with 2× and 4× irradiated powders persisted until the sixth month after irradiation. Figs 4C and 4D show late pathological findings of marked atelectasis and pneumonitis with 2× and 4× radiated powder exposure, respectively, as well as granulomas (Fig. 4E) and severe hemorrhage (Fig. 4F) with 4× radiated powder exposure. Figs 4A and 4B show no pathological findings in the unexposed control and 2.0 Gy γ radiation externally exposed groups, respectively.

Table 2 and Figs 3 and 5 present the pathological findings until 8 months. There was no evidence of hemorrhage or inflammation in the unexposed control and stable Mn groups. The internally exposed group had more emphysema and inflammation than the stable Mn and unexposed control groups. After 8 months, there was no significant difference in collagen deposition, an indicator of conventional fibrosis, between the stable Mn, the internally exposed and the unexposed control groups. However, collagen deposition was significantly higher in the externally exposed group than in the unexposed control group (Figs 5A and C).

Histologically, emphysema is characterized by the destruction of alveolar walls and the enlargement of voids due to apoptosis of lung

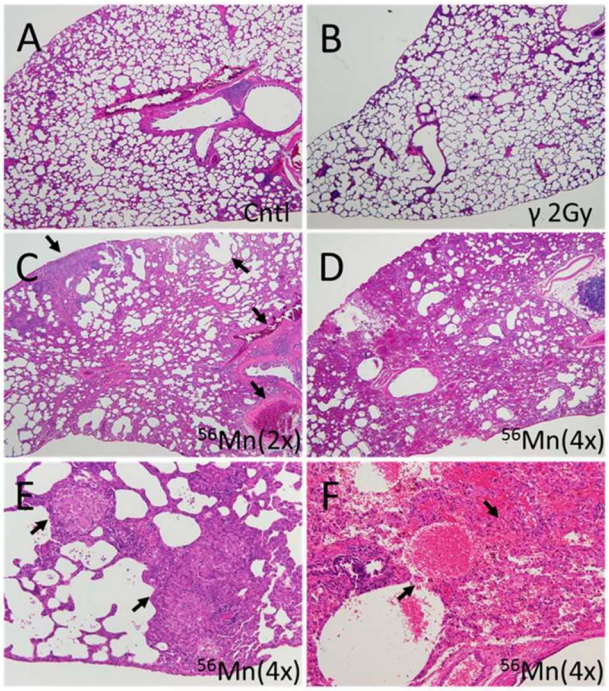

Fig. 4. Representative fields of lung tissue histology from ^{56}Mn-exposed, 2.0-Gy γ-exposed and nonirradiated control rats six months post-irradiation. (A) Lung of a control rat showing no pathological changes; (B) lung of a 2.0-Gy γ-radiation exposed rat showing no pathological changes; (C) lung of a ^{56}Mn(2×) exposed rat showing widespread emphysema, atelectasis, hemorrhage and thrombosis (arrows); (D) lung of a ^{56}Mn(4×) exposed rat showing more extensive damage and pneumonitis due to severe inflammation, inflammatory cell infiltration and intra-alveolar hemorrhage; (E) lung of a ^{56}Mn (4×) exposed rat showing granuloma surrounded by emphysema in a lung lobe (arrows); and (F) lung of a ^{56}Mn (4×) exposed rat showing severe hemorrhage and inflammatory cell infiltration (arrows) and this caption is a higher magnification of caption (D). H&E stain, 4× (A–D) and 20× (E, F) objective magnification (From [6]/CC BY 4.0).

epithelial cells [28], and it is also characterized in humans by oxidative stress, apoptosis and aging due to decreased tissue repair [29, 30].

Radiation pneumonitis has been classified into two phases: early acute pneumonitis and late pulmonary collagen fibrosis [25, 31, 32]. Many tissues, including the lung, dermis and large blood vessels, have elastic properties due to the presence of elastic fibers in the extracellular space, and Rosenbloom *et al.* [33] have demonstrated elastin's crucial role in organ structural integrity. The disrupted structural integrity caused by early stage elastin dysfunction could play a major role in the breakdown of epithelial repair mechanisms, resulting in hemorrhage and emphysema. Loss of elasticity causes age-related phenotypes such as emphysema and arteriosclerosis [34, 35]. External exposure induces collagen fibrosis as a late effect to compensate for the loss of capillaries and alveolar septum due to radiation [32]. On the other hand, as we have shown, because of the local very high-dose exposure, elastin deposition in the extracellular space of the lung and blood vessels is induced as an early effect of internal radiation, resulting in late effects without maintaining the structural integrity of the organs.

In our experiment, three ^{56}Mn 1×, 2× and 4× internally exposed groups demonstrated no difference in alveolar wall thickening and collagen deposition associated with fibrosis. The interstitial tissue was slightly edematous, indicating inflammatory cell infiltration. However, elastin deposition, another pathological indicator of fibrosis, was high in the internally exposed group during the acute to subacute phase, at 6 hours, 3 days, 14 days and 2 months after ^{56}Mn ingestion and the subsequent late phase, at 6 and 8 months after irradiation. Therefore, the 'elastin stigma of internal radiation-induced lung injury was proposed.

The ^{56}Mn internally exposed groups had increased abnormal elastin deposition (elastin stigma). Houghton *et al.* [36] demonstrated that elastin fragments can promote disease progression in a murine model of emphysema. Our findings suggest that the elastin stigma surrounding the alveoli in a staggered distribution, when broken at intervals in ^{56}Mn treated samples as early as six hours, is a predictive indicator of radiation-induced elastin stigma that has occurred in a localized, dose-dependent manner. Therefore, early event data of this elastin stigma, as shown in Figs 3D and 5A–B, may be predictive of late pneumonitis due to internal lung exposure.

LOCALIZED, VERY HIGH DOSE, INTERNAL EXPOSURE

The absorbed dose rates immediately after ^{56}Mn ingestion, cumulative doses in 6 hours, and infinite time from ^{56}Mn particle ingestion are shown in Fig. 6 [6].

Because the half-life of ^{56}Mn is only 2.58 hours, the radioactivity has decayed to 20% after 6 hours, as illustrated in Fig. 6 [6].

The dose rate and cumulative dose due to electrons (β rays) emitted by an activated powder particle depend on its diameter and distance from the center. Larger-diameter particles deliver higher dose rates. At 2.5 μm from the center, the tissue surrounding a 5 μm diameter particle has an absorbed dose rate of 2.70 Gy/hour and a cumulative dose of 8.05 Gy in 6 hours.

The cumulative dose of the tissue is shown in Fig. 7. When the experiment was conducted 6 hours after exposure with a neutron exposure time of 4000 seconds (×2), two masses of activated powder particles were found in the lungs of rats: Shot 1 in the bronchial lumen and Shot 2 in the damaged alveolar necrotic tissue. The cumulative doses at a radial distance of 2.5, 5, 10 and 50 μm from the center of the activated powder particles are 16.1, 2.82, 0.662 and 0.024 Gy, respectively. This is double the amount shown in Fig. 6.

ACTIVATED PARTICLES COEXIST WITH IRON IN BRONCHIAL LUMENS AND DAMAGED NECROTIC ALVEOLAR TISSUE

We present X-ray spectroscopic imaging data from a tissue sample taken 6 hours after inhaling ^{56}Mn in the area of maximal Mn concentration. The method used in this experiment was synchrotron radiation X-ray fluorescence mapping with an X-ray microbeam (SR-XRF), with

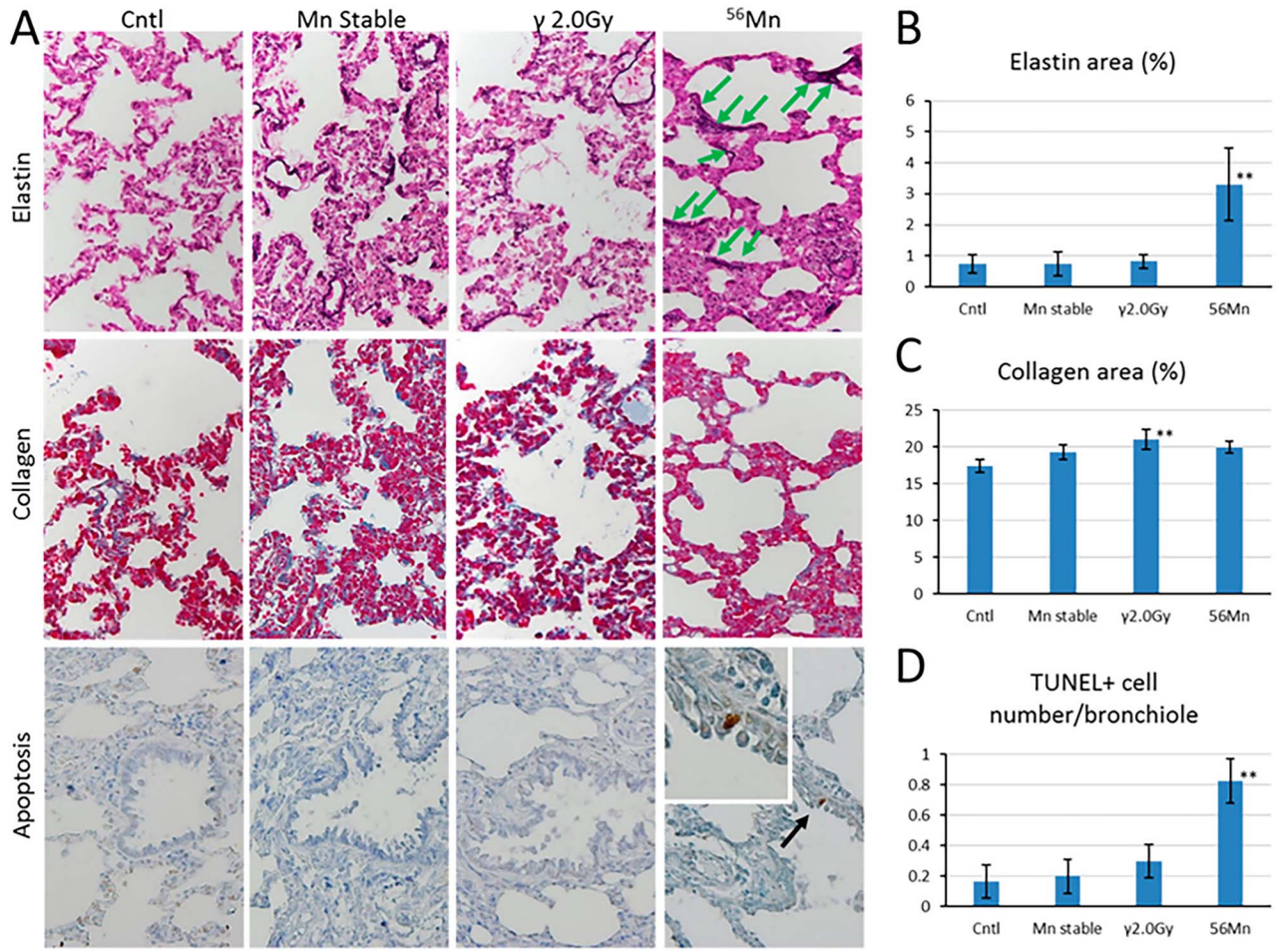

Fig. 5. A comparison of elastin and collagen deposition 8 months and apoptotic frequency 2 months after internal and external radiation exposure to ^{56}Mn (1×). (A) Lung sections from rats were prepared after exposure and evaluated for elastin deposition (purple black) identified by a Verhoeff–Van Gieson stain; collagen deposition (blue) identified by an Azan–Mallory stain; the presence of apoptotic cells (brown, black arrow) in bronchioles identified by a terminal deoxynucleotidyl transferase dUTP nick end labeling stain; and the presence of broken elastin fibers (green arrows); original magnification 40×. Representative images of the control rat (0 Gy), the stable Mn exposure rat, the γ 2.0 Gy irradiated rat (2.0 Gy) and the ^{56}Mn irradiated rat are shown in panels. Radiation-induced changes in percentage elastin area (B), percentage collagen area (C) and number of TUNEL positive cells in bronchioles (D) were determined using cellSens Dimension image acquisition and computer-aided quantification of sampled images. Bars, mean ± standard error of the mean (SEM) (n = 3–6). Significantly different ($^{**}P < 0.01$) from 0 Gy irradiated controls (From [6]/CC BY 4.0).

Mn speciation at the point of interest determined by X-ray absorption near-edge structure (XANES) spectroscopy. The study was performed at the BL-4A station of the High Energy Accelerator Research Organization Photon Factory (KEK-PF, Tsukuba, Japan). Details are provided by Shichijo *et al.* [6]. Shots 1 and 2 were identified as condensed manganese and iron accumulations (Fig. 7). These particles had a valence species of 4 as MnO_2, which changed to divalent after lung tissue deposition (Fig. 7). Inhaling radioactive manganese particles may induce tissue damage, hemorrhage and manganese and iron clots.

EARLY CELLULAR DAMAGE TO LUNG TISSUE FROM INTERNAL RADIATION EXPOSURE IS NON-SPECIFIC, RAPID, SEVERE AND PERSISTENT COMPARED TO EXTERNAL RADIATION EXPOSURE

Pathological changes caused by early cellular damage from internal radiation exposure have a greater impact than that previously reported for experimental animals [16, 17]. While previous studies focused on pathological changes in the lungs caused by external very high doses of more than 8 Gy, our findings showed that internal exposure to a

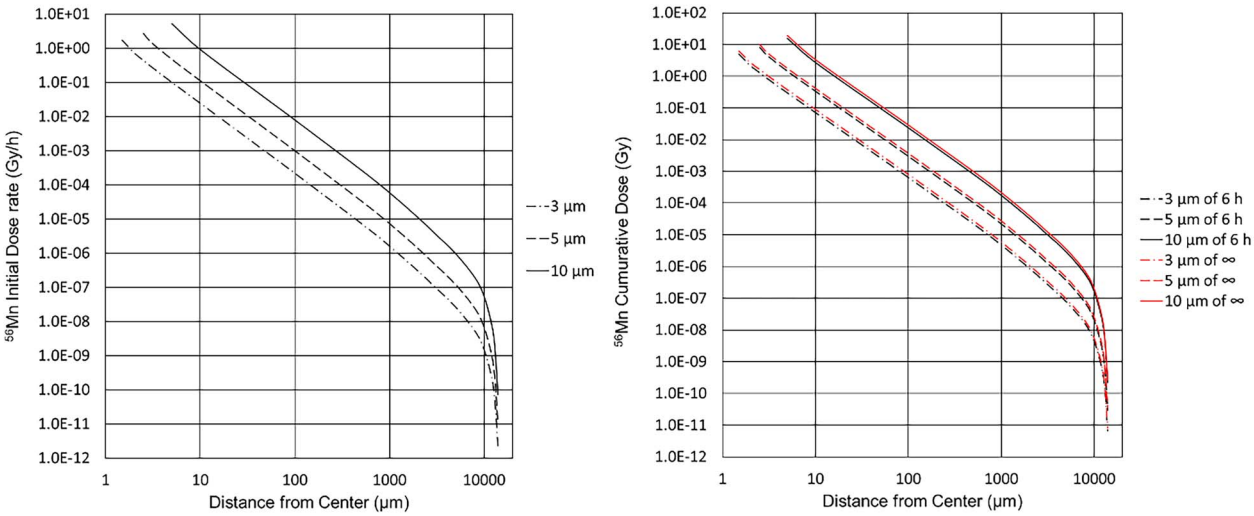

Fig. 6. The absorbed dose rate and the cumulative dose surrounding ^{56}Mn particles of 3, 5 and 10 μm in diameter. The dose rate is measured during inhalation. The cumulative time is 6 hours and infinite time (∞) after inhalation. The irradiated neutrons had a particle fluence of 4×10^{14} n/cm^2 per 2000 seconds of irradiation time, which was irradiated for 2000 seconds ($1\times$) [6].

tissue-averaged dose of 0.10 Gy can cause serious pathological changes in the lungs (Table 1).

The local cumulative dose at the point of proximity to the radioactive particles is 8 Gy, which is a very high dose (Fig. 6) that is likely sufficient to induce pathological changes in the lung tissue. As a deterministic effect of radiation, the threshold for pneumonitis in humans exposed to whole-body external γ-ray has been estimated to be 6 Gy [37]. The pathological findings of internal exposure are dose-dependent and closely related to localized radiation exposure. A new stigma of radiation-induced pneumonitis has been suggested as the interference with epithelial repair mechanisms characterized by high deposition of abnormal elastic fibers (elastin stigma), emphysema and hemorrhage that occur consecutively following an internal radiation exposure. The early onset of these senescence-like effects as a result of localized, very high, internal radiation dose exposure reflects abnormal elastin deposition, along with a disruption of the apoptotic tissue repair mechanisms, as a result of the few lung tissue stem cells [38, 39] in the vicinity of radioactive particles.

Apoptosis-dependent emphysema models have been reported [40, 41], and the apoptotic regulatory system in murine lung injury following high-dose ionizing radiation exposure has already been studied [42, 43]. Because apoptosis was clearly observed in the bronchial epithelial cells of the ^{56}Mn internally exposed group at 2 months, our findings suggest that stem cells, which are thought to reside in bronchial epithelium, are damaged by internal exposure.

According to Liebow *et al.* [44], early Hiroshima A-bomb victims had localized emphysema and atelectasis with or without hemorrhage. The cause of death was presumed to be high doses of external radiation exposure. However, interpreting the cause of emphysema was difficult because it was unknown at the time whether they had received internal radiation exposure. Their data were comparable to ours. Liebow *et al.* [44] reported in Group I, a 13-year-old male who died on the third day. The cause of his hemorrhage was poorly understood, but it was thought to be mainly due to external exposure. Our findings indicate that pulmonary emphysema and hemorrhage can occur in the early stages at relatively low tissue-averaged doses of internal exposure and that doses are not uniform but can be very high locally.

DISCUSSION

The ^{56}Mn-irradiated lung had abnormally high elastin deposition (elastin stigma). In an emphysema murine model, elastin fragments drive disease progression [36]. In addition to high levels of emphysema and hemorrhage, the elastin stigma reveals distinct radiation pathology for internal exposure that differs from the collagen deposition seen with external exposure. In our experiment, early elastin stigma and evidence of apoptosis predicted late effects. Apoptosis in the bronchiole is likely an indicator of stem cell damage [45], resulting in a reduced tissue repair mechanism. Microparticles were found to be condensed manganese and iron accumulations.

International Commission on Radiological Protection (ICRP) defines the equivalent dose to a tissue or organ as the average absorbed dose multiplied by a radiation weighting factor, and this is used as an index for risk assessment [37]. The effects of unequal exposure within tissues or organs are not considered, which may lead to an underestimation of risk for internal exposure involving localized high-dose radiation exposure, as in the preceding case. When a single radioactive particle enters the body, the cells are subjected to concentric circles of internal radiation, resulting in cell death in concentric circles. Cells that are not in the range of radioactive particles survive, while those that were moderately far away from the radiation particles may have survived with their genes damaged. The radioactive microparticles implanted expose the surrounding cells to radiation doses ranging from low to very high. Therefore, detecting the three-dimensional spatial distribution of these internal radiation exposure effects of the implanted radioactive particles is critical.

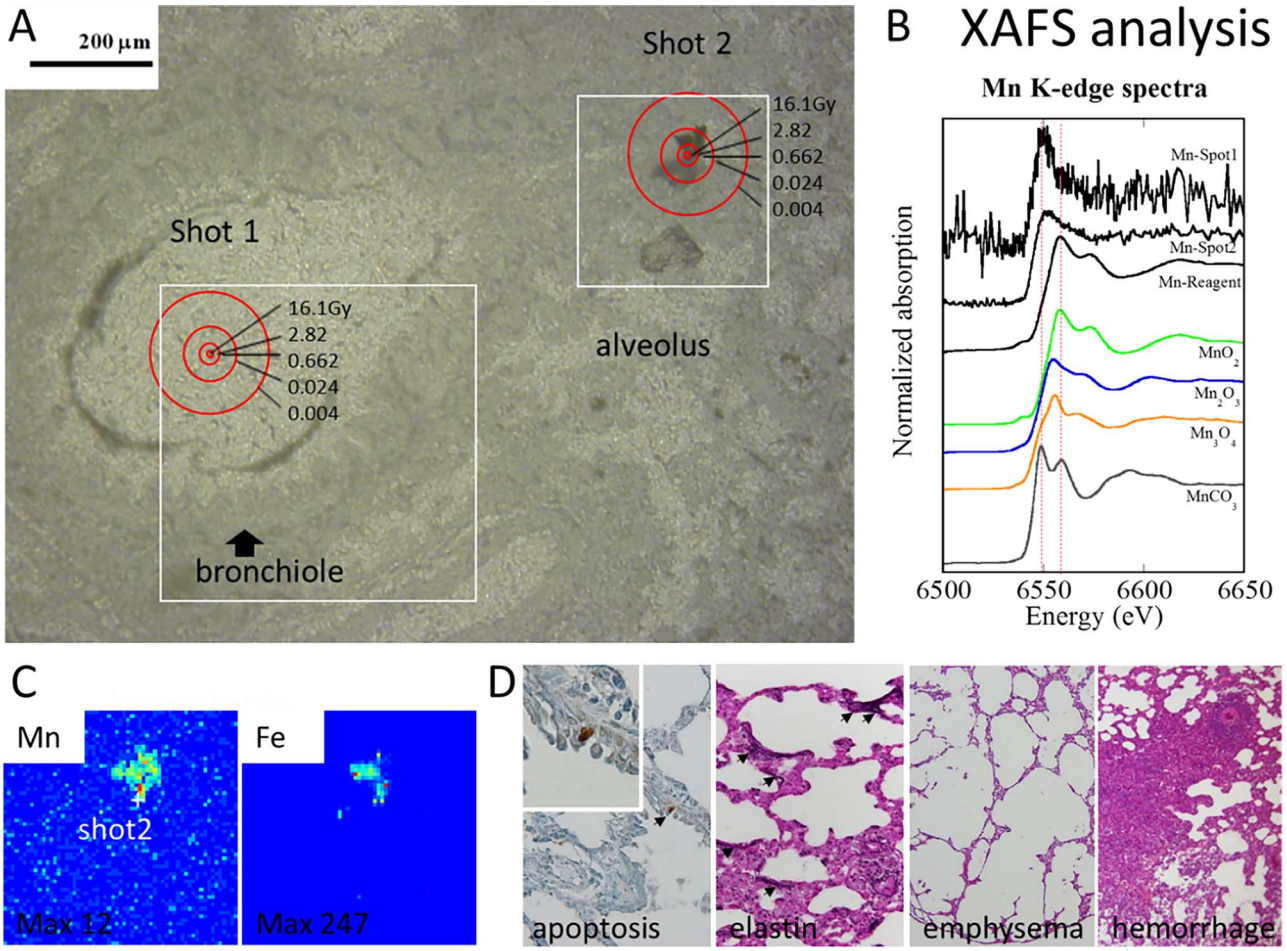

Fig. 7. Cellular damage in lung tissue 6 hours after ^{56}Mn (2×) (A–C) and 2 months after ^{56}Mn (1×) internal exposure (D). (A) Accumulated dose (Gy) in the rat lung tissue surrounding inhaled ^{56}Mn hot particles, (B) X-ray absorption fine structure (XAFS) analysis, (C) condensed manganese and iron accumulations at the hot particle (Shot 2), and (D) apoptosis, elastin stigma, severe emphysema and hemorrhage in the ^{56}Mn internally exposed group (From [6]/CC BY 4.0).

The present experiments demonstrated that internal exposure of tissue to 0.1 Gy causes serious damage, such as hemorrhage, emphysema and atelectasis, whereas external exposure to 2 Gy of ^{60}Co γ radiation causes no such damage. It is difficult to explain the serious damage caused by 0.1 Gy of ^{56}Mn internal exposure, and the reasons and mechanisms of the serious damage caused by radioactive microparticles should be clarified in the future.

ACKNOWLEDGMENTS

The SR-XRF-XANES measurements were performed with the approval of the Photon Factory Program Advisory Committee (proposals no. 2013G052 and 2014G058). We would like to acknowledge the members of the National Nuclear Center of the Republic of Kazakhstan, Almas Azhimkhanov, Vyacheslav Gnyrya and Alexander Kolbayenkov for their support of this work; Aleksey Petukhov and Valeriy Stepanenko of the A. Tsyb Medical Radiological Research Center—National Medical Research Center of Radiology, Ministry of Health of the Russian Federation; Darkhan Uzbekov, Nailya Chaizhunusova, Dariya Shabdarbaeva, Arailym Baurzhan, Gaukhar Amantayeva, Aisulu Saimova, Ynkar Kairkhanova, Bakhyt Ruslanova, Madina Apbassova and Zhaslan Abishev of Semey State Medical University, Republic of Kazakhstan; Minako Kurisu and Yoshio Takahashi of the Department of Earth and Planetary Science, Graduate School of Science of The University of Tokyo; and Masahiro Nakashima and Daisuke Niino of Nagasaki University.

CONFLICTS OF INTEREST

The authors declare that they have no conflict of interest.

FUNDING

This work was supported by the Semey State Medical University, Kazakhstan, Grants-in-Aid for Scientific Research (C) no. 23510064, no. 18 K10027 and no. 21 K10399, KAKENHI to K. Shichijo, and (A) no. 26257501 and (A) no. 19H01149, KAKENHI to M. Hoshi, Japan. This work was also partly supported by the Program of the Network-type Joint Usage/Research Center for Radiation Disaster Medical Science of Hiroshima University, Nagasaki University and Fukushima Medical

University (T19-01-007, T20-01-007, T21-01-014, T22-01-011, respectively).

SUPPLEMENT FUNDING

This work was supported by JSPS KAKENHI Grant Number JP19H01149.

REFERENCES

1. Otani K, Ohtaki M, Yasuda H. Solid cancer mortality risk among a cohort of Hiroshima early entrants after the atomic bombing, 1970–2010: implications regarding health effects of residual radiation. *J Radiat Res* 2022;63(S1):i45–i53.
2. Nagasaki National Peace Memorial Hall for the Atomic Bomb Victims. *Rain: Black Ash and Black Rain*, https://www.peace-nagasaki.go.jp/abombrecords/b020105.html (31 August 2021, date last accessed).
3. Dagle GE, Sanders CL. Radionuclide injury to the lung. *Environ Health Perspect* 1984;55:129–37.
4. Salbu B, Ulanowski A, Fesenko S. IAEA: coordinated research on radioactive particles. *J Environ Radioact* 2021;216:106073, 106111, 106127, 106160.
5. Hoshi M, Stepanenko V, Kaprin A, Ivanov S et al. Overview and analysis of internal radiation dose estimates in experimental animals in a framework of international studies of the sprayed neutron-induced ^{56}Mn radioactive microparticles effects. *J Radiat Res* 2022;63(S1):i8–i15.
6. Shichijo K, Takatsuji T, Abishev Z et al. Impact of local high doses of radiation by neutron activated Mn dioxide powder in rat lungs: protracted pathologic damage initiated by internal exposure. *Biomedicines* 2020;8:171.
7. ICRP. *Dose Coefficients for Intakes of Radionuclides by Workers. ICPR Publication 68, Annals of the ICRP 24*. Oxford: Elsevier Science Ltd., 1994.
8. Ishigure N. Dose quantities used in radiological protection for internal radiation exposure. *Radioisotopes* 2013;62:465–92 (in Japanese).
9. Shichijo K, Takatsuji T, Fukumoto M et al. Autoradiographic analysis of internal plutonium radiation exposure in Nagasaki atomic bomb victims. *Heliyon* 2018;4:e00666.
10. Shichijo K, Takatsuji T, Yamamoto M. Nuclide identification of alpha-emitters by autoradiography in specimen of atomic victims at Nagasaki. In: *Proceedings of the 17th Hiroshima international symposium. IPSHU English research Report Series No. 28, p.70*. Institute for Peace Science, Hiroshima University, 2012.
11. Zeigler JF. *Helium Stopping Powers and Ranges in all Elemental Matter, Volume 4 of the Stopping and Ranges of Ions in Matter*. New York: Pergamon Press, 1977.
12. El Ghissassi F, Baan R, Straif K et al. A review of human carcinogens—part D: radiation. *Lancet Oncol* 2009;10:751–2.
13. Cardis E, Howe G, Ron E et al. Cancer consequences of the Chernobyl accident: 20 years on. *J Radiol Prot* 2006;26:127–40.
14. Adachi K, Kajino M, Zaizen Y et al. Emission of spherical cesium-bearing particles from an early stage of the Fukushima nuclear accident. *Sci Rep* 2013;3:2554.
15. Coggle JE, Lambert BE, Moores SR. Radiation effects in the lung. *Environ Health Perspect* 1986;70:261–91.
16. Ward WF, Kim YT, Molteni A et al. Pentoxifylline does not spare acute radiation reactions in rat lung and skin. *Radiat Res* 1992;129:107–11.
17. Travis EL, Harley RA, Fenn JO et al. Pathologic changes in the lung following single and multi-fraction irradiation. *Int J Radiat Oncol Biol Phys* 1977;2:475–90.
18. Down JD. The nature and relevance of late lung pathology following localized irradiation of the thorax in mice and rats. *Br J Cancer* 1986;7:330–2.
19. Eerde MRV, Kampinga HH, Szabo BG et al. Comparison of three rat strains for development of radiation-induced lung injury after hemithoracic irradiation. *Radiother Oncol* 2001;58:313–6.
20. Stepanenko V, Kaprin A, Ivanov S et al. Microdistribution of internal radiation dose in biological tissues exposed to ^{56}Mn dioxide microparticles. *J Radiat Res* 2022;63(S1):i21–5.
21. Okajima S, Fujita S. Radiation doses from residual radioactivity. In: Roesch W (ed). *U.S. Japan Joint Reassessment of Atomic Bomb Radiation Dosimetry in Hiroshima and Nagasaki; Final Report–Dosimetry System*, Vol. 1. Hiroshima: Radiation Effects Research Foundation, 1987, 205–26 1986 (DS86).
22. Stepanenko V, Rakhypbekov T, Otani K et al. Internal exposure to neutron-activated ^{56}Mn dioxide powder in Wistar rats: part 1: dosimetry. *Radiat Environ Biophys* 2017;56:47–54.
23. Shichijo K, Fujimoto N, Uzbekov D et al. Internal exposure to neutron-activated ^{56}Mn dioxide powder in Wistar rats-part 2: pathological effects. *Radiat Environ Biophys* 2017;56:55–61.
24. Lanin A. *Nuclear Rocket Engine Reactor*. Berlin/Heidelberg: Springer, 2013.
25. Tsoutsou PG, Koukourakis MI. Radiation pneumonitis and fibrosis: mechanisms underlying its pathogenesis and implications for future research. *Int J Radiat Oncol Biol Phys* 2006;66:1281–93.
26. Fujimoto N, Ruslanova B, Abishev Z et al. Biological impacts on the lungs in rats internally exposed to radioactive $^{56}MnO_2$ particle. *Sci Rep* 2021;11:11055.
27. Otani K, Ohtaki M, Fujimoto N et al. Effects of internal exposure to neutron-activated $^{56}MnO_2$ powder on locomotor activity in rats. *J Radiat Res* 2022;63(S1):i38–i44.
28. Hagiyama M, Yoneshige A, Inoue T et al. The intracellular domain of cell adhesion molecule 1 is present in emphysematous lungs and induces lung epithelial cell apoptosis. *J Biomed Sci* 2015;22:67.
29. Christofidou-Solomidou M, Pietrofesa RA, Arguiri E et al. Space radiation-associated lung injury in a murine model. *Am J Physiol Lung Cell Mol Physiol* 2015;308:L416–28.
30. Tuder RM, Petrache I. Pathogenesis of chronic obstructive pulmonary disease. *J Clin Invest* 2012;122:2749–55.
31. Mehta V. Radiation pneumonitis and pulmonary fibrosis in non-small-cell lung cancer: pulmonary function, prediction, and prevention. *Int J Radiat Oncol Biol Phys* 2005;63:5–24.
32. Hanania AN, Mainwaring W, Ghebre YTT et al. Radiation-induced lung injury: assessment and management. *Chest* 2019;156:150–62.

33. Rosenbloom J, Abrams WR, Mecham R. Extracellular matrix 4: the elastic fiber. *FASEB J* 1993;7:1208–18.
34. Pasquali-Ronchetti I, Baccarani-Contri M. Elastic fiber during development and aging. *Microsc Res Tech* 1997;38:428–35.
35. Bailey AJ. Molecular mechanisms of ageing in connective tissues. *Mech Ageing Dev* 2001;122:735–55.
36. Houghton AM, Quintero PA, Perkins DL et al. Elastin fragments drive disease progression in a murine model of emphysema. *J Clin Invest* 2006;116:753–9.
37. ICRP. The 2007 recommendation of the International Commission in Radiological Protection; ICRP Publication 103. *Ann ICRP* Oxford: Elsevier 2007;37:1–332.
38. Kajstura J, Rota M, Hall SR et al. Evidence for human lung stem cells. *N Engl J Med* 2011;364:1795–806.
39. Parekh KR, Nawroth J, Pai A et al. Stem cells and lung regeneration. *Am J Physiol Cell Physiol* 2020;319:C675–93.
40. Diab KJ, Adamowicz JJ, Kamocki K et al. Stimulation of sphingosine 1-phosphate signaling as an alveolar cell survival strategy in emphysema. *Am J Respir Crit Care Med* 2010;181:344–52.
41. Petrache I, Natarajan V, Zhen L et al. Ceramide upregulation causes pulmonary cell apoptosis and emphysema-like disease in mice. *Nat Med* 2005;11:491–8.
42. Kolesnick R, Fuks Z. Radiation and ceramide-induced apoptosis. *Oncogene* 2003;22:5897–906.
43. Mathew B, Jacobson JR, Berdyshev E et al. Role of sphingolipids in murine radiation-induced lung injury: protection by sphingosine 1-phosphate analogs. *FASEB J* 2011;25:3388–400.
44. Liebow AA, Warren S, DeCoursey E. Pathology of atomic bomb casualties. *Am J Pathol* 1949;25:853–1027.
45. Groves AM, Williams JP, Hernady E et al. A potential biomarker for predicting the risk of radiation-induced fibrosis in the lung. *Radiat Res* 2018;190:513–25.